PERGAMON

International Journal of Solids and Structures 37 (2000) 7481–7499

INTERNATIONAL JOURNAL OF SOLIDS and STRUCTURES

www.elsevier.com/locate/ijsolstr

An adaptive finite element algorithm for gradient theory of plasticity with coupling to damage

Thomas Svedberg, Kenneth Runesson *

Department of Solid Mechanics, Chalmers University of Technology, SE-41296 Göteborg, Sweden

Received 6 October 1999; in revised form 1 March 2000

Abstract

In this paper, an adaptive finite element algorithm is proposed for resolving localization zones in plastic solids with coupling to damage, whereby the solution is regularized via the introduction of gradient theory. It is possible to avoid the mesh dependence that otherwise would become inevitable when the localization narrows progressively due to the development of damage. The adaptive method is based on an a posteriori error computation in energy norm for the plastic multiplier based on the constitutive subproblem, which is solved via a mixed finite element formulation. The performance of the proposed method is investigated for a few simple numerical examples in 1D and 2D.

Keywords: Adaptivity; Gradient plasticity; Localization

1. Introduction

Higher order gradients can be introduced in order to regularize the solution pertinent to localization phenomena that appear as discontinuities when the (usual) local continuum formulation is adopted. In mathematical terms, this means that the function space for the displacements is reduced from the space of "bounded variations" (cf. Johnson and Scott, 1981; Temam and Strang, 1980) to a more conventional Hilbert space.

Finite element algorithms, which are based on the truly mixed format in terms of displacements and the plastic multiplier, have been proposed by many authors (Sluys et al., 1993; Pamin, 1994; de Borst and Pamin, 1996; Li and Cescotto, 1996; Comi and Perego, 1996; Comi and Corigliano, 1996). A global variational formulation of gradient theory of damage was proposed by Lorentz and Andrieux (1999). However, due to the high regularity requirements of the plastic multiplier in the used variational formulation(s), the resulting algorithms introduce numerical smearing of the plastic zone when the internal length vanishes. In fact, it is desirable to design the algorithm in such a fashion that the usual algebraic constitutive

* Corresponding author. Tel.: +46-31-771-2478; fax: +46-31-772-3827.
E-mail address: keru@solid.chalmers.se (K. Runesson).

0020-7683/00/$ - see front matter
PII: S0020-7683(00)00208-0

(sub) problem pertinent to local theory is retrieved automatically (as a special case of the general algorithm). In order to avoid the "spurious gradient effect", Svedberg and Runesson (1997, 1998) used a mixed variational format of the constitutive relations, such that piecewise constant approximation of the plastic multiplier can be introduced. It is then possible to solve the equilibrium equation and the constitutive problem in an iterative fashion so that the usual algorithm for the local theory emerges naturally.

As a consequence of the gradient regularization, it is possible to reduce (if not completely avoid) mesh dependence at the finite element (FE) analysis. For problems involving damage, the localization zone width decreases progressively with deformation, and it is found that every (stationary) mesh eventually becomes too coarse to resolve the localization scale. Hence, mesh dependence seems unavoidable. The obvious way to remedy this situation is to adopt an adaptive FE strategy. However, it seems that few (if any) attempts have been made so far to establish a reliable adaptive strategy based on a posteriori error computation in the presence of gradient effects, which is the prime subject of the present paper. Suggestions in the literature concern local continuum theory, which is even more challenging due to the possibility of strong discontinuities. For example, a comparison of error indicators for dynamic localization is found in Belytschko and Tabbara (1993), and *h*-adaptivity in the presence of discontinuities is discussed by Zienkiewicz et al. (1995). The used error indicators are of the heuristic type, i.e. they are not based on an underlying mathematical analysis of the error characteristics for the considered problem type involving localization.

The paper is organized as follows: Section 2 presents the basic constitutive relations involving gradients for a model problem in metal plasticity (based on the von Mises yield criterion). These relations are briefly summarized from Svedberg and Runesson (1997), to which the reader is referred for a comprehensive investigation of the thermodynamic basis. The incremental relations are obtained upon using the fully implicit method for temporal integration. The appropriate mixed variational format of the (incremental) constitutive subproblem is established in Section 3, and the consequent finite element format is established. Due to the nonlinear character of the constitutive relations, a Newton type iterative solution procedure is outlined. Section 4 contains the derivation of an a posteriori error estimate in the (properly defined) energy norm. This estimate is based on a given strain field, i.e. only the constitutive error is included and the equilibrium error(s) are disregarded in the present treatment. An adaptive strategy is also outlined. Finally, the performance of the proposed adaptive algorithm is investigated in a series of numerical examples.

2. Constitutive relations involving gradients – a model problem

2.1. Continuous format

In this paper, we consider a model problem based on the following assumptions: (1) small strain theory with restriction to plane strain, (2) isotropic linear elasticity (for the recoverable part of the deformation), (3) isotropic local damage of Chaboche/Lemaitre type, (4) isotropic local hardening, which is nonlinear of the saturation type, (5) anisotropic linear gradient hardening, and (6) von Mises yield criterion. As a consequence of the introduced assumptions, we may obtain constitutive relations from the proper thermodynamic considerations for the stress $\boldsymbol{\sigma}$, the effective stress $\hat{\boldsymbol{\sigma}}$ and the dissipative stresses K, K^{g} and A (representing local hardening, gradient hardening and damage, respectively) within the given spatial domain Ω:

$$\boldsymbol{\sigma} = (1-\alpha)\hat{\boldsymbol{\sigma}} \quad \text{with} \quad \hat{\boldsymbol{\sigma}}(\boldsymbol{\varepsilon}^{\mathrm{e}}) = \boldsymbol{\mathscr{E}}^{\mathrm{e}} : \boldsymbol{\varepsilon}^{\mathrm{e}}, \quad \boldsymbol{\varepsilon}^{\mathrm{e}} \overset{\mathrm{def}}{=} \boldsymbol{\varepsilon} - \boldsymbol{\varepsilon}^{\mathrm{p}}, \tag{1}$$

$$K(\kappa) = -H\kappa, \tag{2a}$$

$$K^{\mathrm{g}}(\kappa^{\mathrm{g}}) = l^2 \boldsymbol{\nabla} \cdot (\boldsymbol{H}^{\mathrm{g}} \cdot \boldsymbol{\nabla}\kappa^{\mathrm{g}}), \tag{2b}$$

$$A(\boldsymbol{\varepsilon}^{\mathrm{e}}) = \tfrac{1}{2}\boldsymbol{\varepsilon}^{\mathrm{e}} : \boldsymbol{\mathscr{E}}^{\mathrm{e}} : \boldsymbol{\varepsilon}^{\mathrm{e}}, \tag{3}$$

where $\boldsymbol{\varepsilon}(\boldsymbol{u}) = \frac{1}{2}(\boldsymbol{\nabla} \otimes \boldsymbol{u} + \boldsymbol{u} \otimes \boldsymbol{\nabla})$ is the strain (operator), $\boldsymbol{\varepsilon}^{\mathrm{e}}$ and $\boldsymbol{\varepsilon}^{\mathrm{p}}$ are elastic and plastic parts of $\boldsymbol{\varepsilon}$, whereas κ, κ^{g} and α $(0 \leqslant \alpha \leqslant 1)$ are auxiliary internal variables representing local hardening, gradient hardening and damage, respectively. Moreover, $\boldsymbol{\mathscr{E}}^{\mathrm{e}}$ is the fourth-order tensor of constant elastic stiffness moduli; H is the constant (local) hardening modulus, and $\boldsymbol{H}^{\mathrm{g}}$ is the second-order tensor of gradient hardening moduli (that represents anisotropic gradient hardening). Finally, l is the internal length, which is subsequently assumed constant representing a homogeneous micro-structure.

The von Mises yield criterion including gradient effect reads

$$\Phi = \hat{\sigma}_{\mathrm{e}}(\boldsymbol{\varepsilon}^{\mathrm{e}}) - \sigma_{\mathrm{y}} - K(\kappa) - K^{\mathrm{g}}(\kappa^{\mathrm{g}}), \tag{4a}$$

$$\hat{\sigma}_{\mathrm{e}} \overset{\mathrm{def}}{=} \sqrt{\frac{3}{2}}|\hat{\boldsymbol{\sigma}}_{\mathrm{dev}}|, \tag{4b}$$

where σ_{y} is the initial yield stress and $\hat{\sigma}_{\mathrm{e}}$ is the equivalent effective stress.

We shall also need the evolution equations for the internal variables. These are the flow, hardening and damage rules that are given in terms of the plastic multiplier $\dot{\mu}$ as follows:

$$\dot{\boldsymbol{\varepsilon}}^{\mathrm{p}} = \frac{\dot{\mu}}{1-\alpha}\boldsymbol{m}, \qquad \boldsymbol{m}(\boldsymbol{\varepsilon}^{\mathrm{e}}) \overset{\mathrm{def}}{=} \frac{\partial \Phi}{\partial \hat{\boldsymbol{\sigma}}} = \frac{3\hat{\boldsymbol{\sigma}}_{\mathrm{dev}}}{2\hat{\sigma}_{\mathrm{e}}}, \tag{5}$$

$$\dot{\kappa} = -\dot{\mu}\left(1 - \frac{K}{K_{\infty}}\right), \qquad \dot{\kappa}^{\mathrm{g}} = -\dot{\mu}, \tag{6}$$

$$\dot{\alpha} = \dot{\mu}\frac{A(\boldsymbol{\varepsilon}^{\mathrm{e}})}{S(1-\alpha)^{m}}, \tag{7}$$

where K_{∞} is the saturation value of the (local) isotropic hardening, whereas S and m are constitutive parameters that determine the rate of development of damage.

The plastic multiplier is determined by complementary Kuhn–Tucker (KT) conditions:

$$\dot{\mu} \geqslant 0, \quad \Phi \leqslant 0, \quad \dot{\mu}\Phi = 0. \tag{8}$$

Finally, the appropriate boundary condition on $\dot{\mu}$ is of the Neumann type:

$$\boldsymbol{n} \cdot l^2 \boldsymbol{H}^{\mathrm{g}} \cdot \boldsymbol{\nabla}\dot{\mu} = 0, \quad \boldsymbol{x} \in \Gamma, \tag{9}$$

where $\boldsymbol{n}$ is the outward normal to the boundary Γ of Ω.

Remark 1. *Although other boundary conditions are possible* (*admissible*) *from a thermodynamic viewpoint* (*cf.* Svedberg and Runesson, 1997), *the homogeneous condition* (9) *is the only one that will ensure that a bifurcation problem arises from a homogeneous state within* Ω.

2.2. Incremental format from implicit integration

After implicit integration of the rate equations (5)–(7), we obtain the updated values at time t_{n+1} [1] in terms of values at time t_n (indicated by a super-index n):

[1] Super-index $n+1$ is omitted for brevity.

$$\boldsymbol{\varepsilon}^{\mathrm{e}} = {}^{n}\boldsymbol{\varepsilon}^{\mathrm{e,tr}} - \frac{\Delta\mu}{1-\alpha}\boldsymbol{m}(\boldsymbol{\varepsilon}^{\mathrm{e}}) \quad \text{with} \quad {}^{n}\boldsymbol{\varepsilon}^{\mathrm{e,tr}} = \boldsymbol{\varepsilon} - {}^{n}\boldsymbol{\varepsilon}^{\mathrm{p}}, \tag{10}$$

$$\kappa = {}^{n}\kappa - \Delta\mu\left(1 - \frac{K(\kappa)}{K_{\infty}}\right), \tag{11a}$$

$$\kappa^{\mathrm{g}} = {}^{n}\kappa^{\mathrm{g}} - \Delta\mu, \tag{11b}$$

$$\alpha = {}^{n}\alpha + \Delta\mu\frac{A(\boldsymbol{\varepsilon}^{\mathrm{e}})}{S(1-\alpha)^{m}}. \tag{12}$$

The incremental format of Eq. (8) is

$$\Delta\mu \geqslant 0, \quad \Phi \leqslant 0, \quad \Delta\mu\Phi = 0. \tag{13}$$

Due to the linear character of the gradient hardening, we may eliminate κ^{g} by inserting Eq. 11b into Eq. 4a and using Eq. 2b to obtain

$$\Phi = -f(\boldsymbol{\varepsilon}^{\mathrm{e}}, \kappa) + l^{2}\boldsymbol{\nabla}\cdot(\boldsymbol{H}^{\mathrm{g}}\cdot\boldsymbol{\nabla}(\Delta\mu)), \tag{14}$$

where we introduced the notation

$$f(\boldsymbol{\varepsilon}^{\mathrm{e}}, \kappa) = -\hat{\sigma}_{\mathrm{e}}(\boldsymbol{\varepsilon}^{\mathrm{e}}) + \sigma_{\mathrm{y}} - H\kappa + {}^{n}K^{\mathrm{g}}. \tag{15}$$

We remark that the last term of $f(\boldsymbol{\varepsilon}^{\mathrm{e}}, \kappa)$ stems from the gradient effect.

Because of the nonlinear character of Eqs. (10)–(14), we rewrite these equations in terms of residuals that must vanish (whereby we make the change of notation $\Delta\mu \rightarrow \mu$ for brevity):

$$\boldsymbol{R}_{\varepsilon}(\mu; \boldsymbol{\varepsilon}^{\mathrm{e}}, \alpha) = \boldsymbol{\varepsilon}^{\mathrm{e}} - {}^{n}\boldsymbol{\varepsilon}^{\mathrm{e,tr}} + \frac{\mu}{1-\alpha}\boldsymbol{m}(\boldsymbol{\varepsilon}^{\mathrm{e}}) = 0, \tag{16}$$

$$R_{\kappa}(\mu; \kappa) = \kappa - {}^{n}\kappa + \mu\left(1 - \frac{K(\kappa)}{K_{\infty}}\right) = 0, \tag{17}$$

$$R_{\alpha}(\mu; \boldsymbol{\varepsilon}^{\mathrm{e}}, \alpha) = \alpha - {}^{n}\alpha - \mu\frac{A(\boldsymbol{\varepsilon}^{\mathrm{e}})}{S(1-\alpha)^{m}} = 0, \tag{18}$$

$$R_{\mu}(\mu; \boldsymbol{\varepsilon}^{\mathrm{e}}, \kappa) = -l^{2}\boldsymbol{\nabla}\cdot(\boldsymbol{H}^{\mathrm{g}}\cdot\boldsymbol{\nabla}\mu) + f(\boldsymbol{\varepsilon}^{\mathrm{e}}, \kappa) + \Phi = 0. \tag{19}$$

We remark that it is only Eq. (19) that involves any gradient effect; Eqs. (16)–(18) are the same as in the local theory.

We shall henceforth consider a more compact formulation of Eqs. (16)–(19) by introducing $\boldsymbol{q} \overset{\mathrm{def}}{=} [\boldsymbol{\varepsilon}^{\mathrm{e}}, \kappa, \alpha]^{\mathrm{T}}$ as the column matrix containing all the components of $\boldsymbol{\varepsilon}^{\mathrm{e}}$ in addition to κ and α. The corresponding residual matrix is $\boldsymbol{R}_{\boldsymbol{q}} = [\boldsymbol{R}_{\varepsilon}, R_{\kappa}, R_{\alpha}]^{\mathrm{T}}$.

Remark 2. *The vectors* $\boldsymbol{q}$ *and* $\boldsymbol{R}_{\boldsymbol{q}}$ *can be extended to include more variables if this is found necessary* (*or otherwise convenient*) *from modeling or numerical reasons.*

Moreover, we shall complement the problem formulation with the KT-conditions (13) and the appropriate boundary condition to give the problem:

$$\boldsymbol{R}_{\boldsymbol{q}}(\mu; \boldsymbol{q}) = 0 \quad \text{in } \Omega, \tag{20}$$

$$R_{\mu}(\mu; \boldsymbol{q}) = -l^{2}\boldsymbol{\nabla}\cdot(\boldsymbol{H}^{\mathrm{g}}\cdot\boldsymbol{\nabla}\mu) + f(\mu; \boldsymbol{q}) + \Phi = 0 \quad \text{in } \Omega, \tag{21}$$

$$\mu \geqslant 0, \quad \Phi \leqslant 0, \quad \mu\Phi = 0 \quad \text{in } \Omega, \tag{22}$$

$$\boldsymbol{n} \cdot l^2 \boldsymbol{H}^{\mathrm{g}} \cdot \nabla \mu = 0 \quad \text{on } \Gamma. \tag{23}$$

Let us, next, consider the special case of local theory, defined by $l = 0$, in which case the problem is completely algebraic and can be solved for each $\boldsymbol{x} \in \Omega$ independently. Hence, we obtain for $\boldsymbol{x} \in \Omega$

$$\boldsymbol{R}_{\boldsymbol{q}}(\mu; \boldsymbol{q}) = 0, \tag{24}$$

$$R_{\mu}(\mu; \boldsymbol{q}) = f(\mu; \boldsymbol{q}) + \Phi = 0, \tag{25}$$

$$\mu \geqslant 0, \quad \Phi \leqslant 0, \quad \mu\Phi = 0. \tag{26}$$

The problem is solved as follows: Check loading (L) or unloading (U) by setting $\mu = 0$ to obtain the "trial" value $\boldsymbol{q} = \boldsymbol{q}^{\mathrm{tr}}$ from $\boldsymbol{R}_{\boldsymbol{q}}(0; \boldsymbol{q}^{\mathrm{tr}}) = 0$ in Eq. (24). We then obtain the trial value $\Phi^{\mathrm{tr}} = -f(0; \boldsymbol{q}^{\mathrm{tr}})$ from Eq. (25), whereby the KT-conditions (26) give two possibilities:
1. if $\Phi^{\mathrm{tr}} \leqslant 0$, then (U),
2. if $\Phi^{\mathrm{tr}} > 0$, then (L) since $\mu = 0$ is not possible.

3. Mixed variational format of constitutive problem

3.1. Strong and variational formulations

For reasons that were discussed in Section 1 (cf. Svedberg and Runesson, 1997), it is desirable to introduce a special mixed FE-formulation of the constitutive problem (20)–(23). On introducing the gradient

$$\boldsymbol{g} = \boldsymbol{H}^{\mathrm{g}} \cdot \nabla \mu, \tag{27}$$

we replace Eqs. (20)–(23) by

$$\boldsymbol{R}_{\boldsymbol{q}}(\mu; \boldsymbol{q}) = 0 \quad \text{in } \Omega, \tag{28}$$

$$R_{\mu}(\mu, \boldsymbol{g}; \boldsymbol{q}) = -l^2 \nabla \cdot \boldsymbol{g} + f(\mu; \boldsymbol{q}) + \Phi = 0 \quad \text{in } \Omega, \tag{29}$$

$$\boldsymbol{R}_{\boldsymbol{g}}(\mu, \boldsymbol{g}) = (\boldsymbol{H}^{\mathrm{g}})^{-1} \cdot \boldsymbol{g} - \nabla \mu = 0 \quad \text{in } \Omega, \tag{30}$$

$$\mu \geqslant 0, \quad \Phi \leqslant 0, \quad \mu\Phi = 0 \quad \text{in } \Omega, \tag{31}$$

$$\boldsymbol{n} \cdot \boldsymbol{g} = 0 \quad \text{on } \Gamma. \tag{32}$$

Next, we introduce a variational format that admits μ to be approximated (in the subsequent FE-formulation) as piecewise constant. In order to do so, we first define usual scalar product and norm in the L_2-metric for $u, u' \in L_2(\Omega)$

$$(u, u') = (u, u')_{L_2(\Omega)} \stackrel{\mathrm{def}}{=} \int_{\Omega} u u' \, \mathrm{d}\Omega, \quad \|u\| \stackrel{\mathrm{def}}{=} \sqrt{(u, u)} \tag{33}$$

and the "complementary energy" product and corresponding norm for $\boldsymbol{g}$

$$(\boldsymbol{g}, \boldsymbol{g}')_C \stackrel{\mathrm{def}}{=} \int_{\Omega} \boldsymbol{g} \cdot (\boldsymbol{H}^{\mathrm{g}})^{-1} \cdot \boldsymbol{g}' \, \mathrm{d}\Omega, \quad \|\boldsymbol{g}\|_C \stackrel{\mathrm{def}}{=} \sqrt{(\boldsymbol{g}, \boldsymbol{g})_C}. \tag{34}$$

The proper spaces are

$$V = L_2(\Omega), \qquad V^+ = \{\mu \in V, \mu \geqslant 0 \text{ in } \Omega\}, \tag{35}$$

$$W = \left\{ \boldsymbol{g} \in [L_2(\Omega)]^2, \boldsymbol{n} \cdot \boldsymbol{g} = 0 \text{ on } \Gamma \right\}. \tag{36}$$

Remark 3. *The condition $\boldsymbol{n} \cdot \boldsymbol{g} = 0$, which is usually considered as a natural condition, is an essential boundary condition in the proposed variational format.*

The proposed variational format of Eqs. (28)–(31) is as follows: Find $\mu \in V^+$ and $\boldsymbol{g} \in W$ such that

$$-(\Phi, \mu' - \mu) \geqslant 0 \quad \forall \mu' \in V^+, \tag{37}$$

$$(\boldsymbol{g}, \boldsymbol{g}')_C + (\mu, \nabla \cdot \boldsymbol{g}') = 0 \quad \forall \boldsymbol{g}' \in W \tag{38}$$

subjected to the conditions

$$\boldsymbol{R}_{\boldsymbol{q}}(\mu; \boldsymbol{q}) = 0, \tag{39}$$

$$R_\mu(\mu, \boldsymbol{g}; \boldsymbol{q}) = 0. \tag{40}$$

It follows by inspection that Eq. (37) is identical to Eq. (31), and Φ can be eliminated in terms of μ, $\boldsymbol{g}$ and $\boldsymbol{q}$ from Eq. (40). Finally, Eq. (38) is the variational format of Eq. (30), which is a linear relation in μ and $\boldsymbol{g}$.

Due to the nonlinear character of the problem, we find it more convenient to treat Φ as an independent variable. Moreover, we may (formally) solve for $\boldsymbol{q} = \boldsymbol{q}(\mu)$ from Eq. (39), [2] and we introduce the auxiliary space

$$V^- = \{\Phi \in V, \Phi \leqslant 0 \text{ in } \Omega\}, \tag{41}$$

whereby the problem is slightly rephrased: Find $\mu \in V$, $\Phi \in V^-$, and $\boldsymbol{g} \in W$ such that

$$(R_\mu, \mu') = 0 \quad \forall \mu' \in V, \qquad R_\mu \stackrel{\text{def}}{=} -l^2 \nabla \cdot \boldsymbol{g} + f(\mu; \boldsymbol{q}(\mu)) + \Phi, \tag{42}$$

$$(\boldsymbol{R}_{\boldsymbol{g}}, \boldsymbol{g}') \stackrel{\text{def}}{=} (\boldsymbol{g}, \boldsymbol{g}')_C + (\mu, \nabla \cdot \boldsymbol{g}') = 0 \quad \forall \boldsymbol{g}' \in W, \tag{43}$$

$$(\mu, \Phi' - \Phi) \geqslant 0 \quad \forall \Phi' \in V^-. \tag{44}$$

From the solution of Eq. (37), or Eq. (44), we define the *current* loading region $\Omega^{(\mathrm{L})}$ and unloading region $\Omega^{(\mathrm{U})}$, with $\Omega = \Omega^{(\mathrm{L})} \cup \Omega^{(\mathrm{U})}$, as follows:

$$\Omega^{(\mathrm{L})} = \{\boldsymbol{x} \in \Omega, \mu(\boldsymbol{x}) > 0, \Phi(\boldsymbol{x}) = 0\}, \tag{45}$$

$$\Omega^{(\mathrm{U})} = \{\boldsymbol{x} \in \Omega, \mu(\boldsymbol{x}) = 0, \Phi(\boldsymbol{x}) \leqslant 0\}. \tag{46}$$

3.2. Mixed finite element approximation

In order to be specific, we introduce $\mathscr{M}_h = \{\Omega_e\}$ as a standard FE subdivision (or mesh) of triangular elements (in 2D). The diameter of each element is denoted by h_e. We shall consider $h(\boldsymbol{x})$ as a function on Ω, defining the local mesh size, such that $h(\boldsymbol{x}) = h_e$ when $\boldsymbol{x} \in \Omega_e$.

On introducing subspaces $V_h \subset V$, $V_h^- \subset V^-$ and $W_h \subset W$, we can now formulate the Galerkin version of Eqs. (42)–(44) as follows: Find $\mu_h \in V_h$, $\Phi_h \in V_h^-$, and $\boldsymbol{g}_h \in W_h$ such that

[2] In practice, this solution must be obtained by iteration and is given later.

$$(R^h_\mu, \mu'_h) = 0 \quad \forall \mu'_h \in V_h, \qquad R^h_\mu = -l^2 \nabla \cdot \boldsymbol{g}_h + f(\mu_h; \boldsymbol{q}(\mu_h)) + \Phi_h, \tag{47}$$

$$(\boldsymbol{R}^h_{\boldsymbol{g}}, \boldsymbol{g}'_h) \overset{\text{def}}{=} (\boldsymbol{g}_h, \boldsymbol{g}'_h)_C + (\mu_h, \nabla \cdot \boldsymbol{g}'_h) = 0 \quad \forall \boldsymbol{g}'_h \in W_h, \tag{48}$$

$$(\mu_h, \Phi'_h - \Phi_h) \geqslant 0 \quad \forall \Phi'_h \in V_h^-. \tag{49}$$

We may also establish the Galerkin-orthogonality relations, which are obtained as follows: Set $\mu' = \mu'_h \in V_h$ in Eq. (42) and $\boldsymbol{g}' = \boldsymbol{g}'_h \in W_h$ in Eq. (43). Subtract Eqs. (47) and (48) from the resulting expression to obtain

$$\left(- l^2 \nabla \cdot \boldsymbol{e}_{\boldsymbol{g}} + f(\mu; q(\mu)) - f(\mu_h; q(\mu_h)) + \Phi - \Phi_h, \mu'_h \right) = 0 \quad \forall \mu'_h \in V_h, \tag{50}$$

$$(\boldsymbol{e}_{\boldsymbol{g}}, \boldsymbol{g}'_h)_C + (e_\mu, \nabla \cdot \boldsymbol{g}'_h) = 0 \quad \forall \boldsymbol{g}'_h \in W_h, \tag{51}$$

where we introduced the errors in μ and $\boldsymbol{g}$ as

$$e_\mu = \mu - \mu_h, \qquad \boldsymbol{e}_{\boldsymbol{g}} = \boldsymbol{g} - \boldsymbol{g}_h. \tag{52}$$

Subsequently, we shall in particular be concerned with the approximation (CL) defined as follows: V_h consists of piecewise constants (which are clearly discontinuous across element boundaries), whereas W_h consists of piecewise linears, which are continuous. For this choice, we assume that ${}^n\boldsymbol{\varepsilon}^{\text{tr}} \in V_h$. It then follows that $\boldsymbol{q}(\mu_h) \in V_h$ and, hence, $f(\mu_h; \boldsymbol{q}(\mu_h)) \in V_h$. We thus conclude that $R^h_\mu \in V_h$, and from the variational statement (47) follows that the finite element solution must be "residual-free" in the sense that $R^h_\mu = 0$ in Ω.

Remark 4. *Since* $R^h_\mu = 0$, *there is no error from Eq.* (47) *or Eq.* (49); *hence*, *the complete error comes from Eq.* (48).

3.3. Iterative solution procedure

Since R_μ is a nonlinear function of μ and $\boldsymbol{g}$, it is only at convergence of a suitably chosen iteration algorithm that $R^h_\mu = 0$. We may employ Newton iterations to solve for μ_h and $\boldsymbol{g}_h$ from the relations

$$R_\mu(\mu_h, \boldsymbol{g}_h) = -l^2 \nabla \cdot \boldsymbol{g}_h + f(\mu_h; \boldsymbol{q}_h) + \Phi_h = 0, \quad \boldsymbol{x} \in \Omega, \tag{53}$$

$$(\boldsymbol{g}_h, \boldsymbol{g}'_h)_C + (\mu_h, \nabla \cdot \boldsymbol{g}'_h) = 0 \quad \forall \boldsymbol{g}'_h \in W_h \tag{54}$$

subjected to the conditions

$$\mu_h \geqslant 0, \quad \Phi_h \leqslant 0, \quad \mu_h \Phi_h = 0, \quad \boldsymbol{x} \in \Omega, \tag{55}$$

$$\boldsymbol{R}_{\boldsymbol{q}}(\mu_h; \boldsymbol{q}_h) = 0. \tag{56}$$

Remark 5. *Since* $\mu^h(\boldsymbol{x}) = \mu_{h,e}$, $\Phi_h(\boldsymbol{x}) = \Phi_{h,e}$, $\boldsymbol{q}^h(\boldsymbol{x}) = \boldsymbol{q}_{h,e}$ for $e = 1, 2, \ldots, N$ (*where* N *is the number of elements in the current mesh* $\mathscr{M}_h$), *it appears that Eqs.* (53), (55) and (56) *represent element relations.*

Upon linearizing $\boldsymbol{R}_{\boldsymbol{q}}(\mu; \boldsymbol{q}) = 0$, we first obtain

$$\mathrm{d}\boldsymbol{q} = \left(\boldsymbol{J}_{\boldsymbol{q}}\right)^{-1} \left(\mathrm{d}\boldsymbol{R}_{\boldsymbol{q}} - \boldsymbol{J}_\mu \mathrm{d}\mu\right), \tag{57}$$

where we introduced the Jacobian matrices

$$\boldsymbol{J}_{\boldsymbol{q}} \overset{\text{def}}{=} \frac{\partial \boldsymbol{R}_{\boldsymbol{q}}}{\partial \boldsymbol{q}}, \qquad \boldsymbol{J}_\mu \overset{\text{def}}{=} \frac{\partial \boldsymbol{R}_{\boldsymbol{q}}}{\partial \mu}. \tag{58}$$

Inserting Eq. (57) into the linearized version of Eq. (53), we obtain

$$-l^2\nabla\cdot \mathrm{d}\boldsymbol{g}_h + h\,\mathrm{d}\mu_h = \boldsymbol{s}^{\mathrm{T}}\,\mathrm{d}\boldsymbol{R}_{\boldsymbol{q}} - \mathrm{d}\Phi_h + \mathrm{d}R_\mu, \tag{59}$$

where we introduced the notation

$$h \overset{\text{def}}{=} \frac{\partial f}{\partial \mu} + \boldsymbol{s}^{\mathrm{T}}\boldsymbol{J}_\mu, \qquad \boldsymbol{s} \overset{\text{def}}{=} -\left(\boldsymbol{J}_{\boldsymbol{q}}\right)^{-\mathrm{T}}\frac{\partial f}{\partial \boldsymbol{q}}. \tag{60}$$

Remark 6. *If we consider $f = f(\mu;\boldsymbol{q}(\mu))$, then*

$$h \overset{\text{def}}{=} \frac{\mathrm{d}f}{\mathrm{d}\mu}, \tag{61}$$

i.e. h is the Jacobian of f. We shall assume that $h > 0$ for all possible values of the argument μ.

On setting $\mathrm{d}\mu := \mu^{(k)} - \mu^{(k-1)}$, $\mathrm{d}\boldsymbol{g}_h := \boldsymbol{g}_h^{(k)} - \boldsymbol{g}_h^{(k-1)}$, $\mathrm{d}\Phi_h := \Phi_h^{(k)} - \Phi_h^{(k-1)}$, $\mathrm{d}R_\mu := -R_\mu^{h(k-1)}$, $\mathrm{d}\boldsymbol{R}_{\boldsymbol{q}} := -\boldsymbol{R}_{\boldsymbol{q}}^{h(k-1)}$ and inserting these expressions into Eq. (59), we obtain the following mixed finite element problem to be solved in each Newton step (k):

$$-l^2\nabla\cdot\boldsymbol{g}_h^{(k)} + h^{(k-1)}\mu_h^{(k)} = \Phi_h^{\mathrm{tr}(k-1)} - \Phi_h^{(k)}, \tag{62}$$

$$(\boldsymbol{g}_h^{(k)}, \boldsymbol{g}_h')_C + (\mu_h^{(k)}, \nabla\cdot\boldsymbol{g}_h') = 0 \quad \forall \boldsymbol{g}_h' \in W_h, \tag{63}$$

$$\mu_h^{(k)} \geqslant 0, \quad \Phi_h^{(k)} \leqslant 0, \quad \mu_h^{(k)}\Phi_h^{(k)} = 0, \tag{64}$$

where we introduced the "trial value" of Φ as follows:

$$\Phi_h^{\mathrm{tr}} \overset{\text{def}}{=} -R_\mu^h + \Phi_h - \boldsymbol{s}^{\mathrm{T}}\boldsymbol{R}_{\boldsymbol{q}}^h - l^2\nabla\cdot\boldsymbol{g}_h + h\mu_h. \tag{65}$$

How to solve for $\mu_h^{(k)}$, $\boldsymbol{g}_h^{(k)}$ and $\Phi_h^{(k)}$ in each iteration from Eqs. (62)–(64) in an efficient manner was discussed in some detail by Svedberg and Runesson, 1998; however, as part of a more restrictive setting. When $\mu^{(k)}$ is known, it is possible to update $\boldsymbol{q}$:

$$\boldsymbol{q}^{(k)} = \boldsymbol{q}^{(k-1)} + \left(\boldsymbol{J}_{\boldsymbol{q}}^{(k-1)}\right)^{-1}\left[-\boldsymbol{R}_{\boldsymbol{q}}^{h(k-1)} - \boldsymbol{J}_\mu^{h(k-1)}\left(\mu^{(k)} - \mu^{(k-1)}\right)\right]. \tag{66}$$

The iteration algorithm for the constitutive sub (problem) is summarized below.

- $k = 0$:
  1. Set $\mu_h^{(0)} = 0$, $\boldsymbol{g}_h^{(0)} = 0$, $\Phi_h^{(0)} = 0$.
  2. Get "trial state" $\boldsymbol{q}_h^{(0)}$ from $\boldsymbol{R}_{\boldsymbol{q}}^h(0, \boldsymbol{q}_h^{(0)}) = 0$.
  3. Calculate $R_\mu^{h(0)}$.
- $k > 0$:
  1. Calculate $\Phi_h^{\mathrm{tr}(k-1)}$ and $h^{(k-1)}$.
  2. Solve for $\mu_h^{(k)}$, $\boldsymbol{g}_h^{(k)}$, $\Phi_h^{(k)}$ from

$$\begin{cases} -l^2\nabla\cdot\boldsymbol{g}_h^{(k)} + h^{(k-1)}\mu^{(k)} = \Phi_h^{\mathrm{tr}(k-1)} - \Phi_h^{(k)}, \\ \mu^{(k)} \geqslant 0, \quad \Phi_h^{(k)} \leqslant 0, \quad \mu^{(k)}\Phi_h^{(k)} = 0. \end{cases}$$

  3. Calculate the updated value $\boldsymbol{q}_h^{(k)}$ from Eq. (66).
  4. Calculate $R_\mu^{h(k)}$ and $\boldsymbol{R}_{\boldsymbol{q}}^{h(k)}$.
  5. Check residuals against given tolerance, if not fulfilled, $k \to k+1$ and continue iteration.

4. A posteriori error estimate and adaptive strategy

4.1. Preliminaries

Subsequently, we shall establish a posteriori error estimates in the (suitably defined) energy norm. In order to avoid excessive complexity, we introduce the simplifying assumption that $\Omega_h^{(\mathrm{L})} = \Omega^{(\mathrm{L})}$ (and $\Omega_h^{(\mathrm{U})} = \Omega^{(\mathrm{U})}$). This means that $\Phi = \Phi_h = 0$ in $\Omega^{(\mathrm{L})}$, whereas $\mu = \mu_h = 0$ in $\Omega^{(\mathrm{U})}$. Hence, $e_\mu = 0$, $\boldsymbol{e}_{\boldsymbol{g}} = 0$ in $\Omega^{(\mathrm{U})}$ and $\Omega^{(\mathrm{L})}$ is the only region of interest. For the error analysis, it is then sufficient to set $\Phi_h = 0$ in Eq. (47) and to consider the (slightly simplified) problem of finding $\mu_h \in V_h$ and $\boldsymbol{g}_h \in W_h$ such that

$$(R_\mu^h, \mu_h') = 0 \quad \forall \mu_h' \in V_h, \qquad R_\mu^h = -l^2 \nabla \cdot \boldsymbol{g}_h + f(\mu_h; \boldsymbol{q}(\mu_h)), \tag{67}$$

$$(\boldsymbol{g}_h, \boldsymbol{g}_h')_C + (\mu_h, \nabla \cdot \boldsymbol{g}_h') = 0 \quad \forall \boldsymbol{g}_h' \in W_h. \tag{68}$$

We shall also introduce the operator $A(\mu, \mu_h)$ defined by

$$A(\mu, \mu_h) \overset{\text{def}}{=} \int_0^1 \frac{\mathrm{d}f}{\mathrm{d}\mu^*}(\mu^*(s); \boldsymbol{q}(\mu^*(s)))\mathrm{d}s, \qquad \mu^*(s) = s\mu + (1-s)\mu_h, \tag{69}$$

which has the useful property (cf. Eriksson et al., 1995)

$$Ae_\mu = \int_0^1 \frac{\mathrm{d}}{\mathrm{d}s} f(\mu^*(s); \boldsymbol{q}(\mu^*(s)))\mathrm{d}s = f(\mu; \boldsymbol{q}(\mu)) - f(\mu_h; \boldsymbol{q}(\mu_h)). \tag{70}$$

Remark 7. *In practice, we may evaluate A approximately as follows*:

$$A \simeq \frac{\mathrm{d}f}{\mathrm{d}\mu^*}(\mu^*(0); \boldsymbol{q}(\mu^*(0))) = \frac{\mathrm{d}f}{\mathrm{d}\mu}(\mu_h; \boldsymbol{q}(\mu_h)) = h(\mu_h), \tag{71}$$

i.e. A can be computed as the Jacobian of f at $\mu = \mu_h$.

We also introduce the norm associated with A: For $u \in L_2(\Omega)$, we define

$$\|u\|_A = \sqrt{(Au, u)}. \tag{72}$$

Since $h > 0$, it follows that $\|\cdot\|_A$ is indeed a norm.

4.2. Error estimate in energy norm

We define the error in the energy norm $e_{\mathrm{E}}(\mu_h, \boldsymbol{g}_h)$ as follows:

$$e_{\mathrm{E}}^2 \overset{\text{def}}{=} l^2 \|\boldsymbol{e}_{\boldsymbol{g}}\|_C^2 + \|e_\mu\|_A^2 = l^2(\boldsymbol{e}_{\boldsymbol{g}}, \boldsymbol{e}_{\boldsymbol{g}})_C + (Ae_\mu, e_\mu). \tag{73}$$

Now, subtracting and adding the term $l^2(\nabla \cdot e_{\boldsymbol{g}}, e_\mu)$ and using the property Eq. 70 of A, we may rewrite Eq. (73) as

$$e_{\mathrm{E}}^2 = -(\hat{R}_1, e_\mu) + l^2(\boldsymbol{e}_{\boldsymbol{g}}, \boldsymbol{e}_{\boldsymbol{g}})_C + l^2(e_\mu, \nabla \cdot \boldsymbol{e}_{\boldsymbol{g}}), \tag{74}$$

where we introduced the notation $\hat{R}_1 = R_\mu(\mu_h, \boldsymbol{g}_h)$. Integrating the last term in Eq. (74) by parts on each Ω_e and collecting terms, we obtain the (exact) error representation

$$e_{\mathrm{E}}^2 = \sum_{e=1}^{N} \left(E_{1,e} + E_{2,e} + E_{2,e}^{\mathrm{in}} \right), \tag{75}$$

where the element contributions to the error are

$$E_{1,e} = -\int_{\Omega_e} \hat{R}_1 e_\mu \,\mathrm{d}\Omega, \qquad \hat{R}_1(\mu_h, \boldsymbol{g}_h) = -l^2 \nabla \cdot \boldsymbol{g}_h + f(\mu_h; \boldsymbol{q}(\mu_h)), \tag{76}$$

$$E_{2,e} = -l^2 \int_{\Omega_e} \hat{\boldsymbol{R}}_2 \cdot \boldsymbol{e}_g \,\mathrm{d}\Omega, \qquad \hat{\boldsymbol{R}}_2(\mu_h, \boldsymbol{g}_h) = (\boldsymbol{H}^{\mathrm{g}})^{-1} \cdot \boldsymbol{g}_h - \nabla \mu_h, \tag{77}$$

$$E^{\mathrm{in}}_{2,e} = -l^2 \int_{\Gamma^{\mathrm{in}}_e} h_e \hat{R}^{\mathrm{in}}_2 \boldsymbol{n} \cdot \boldsymbol{e}_g \,\mathrm{d}\Gamma, \qquad \hat{R}^{\mathrm{in}}_2(\mu_h) = -\frac{1}{2h_e}[[\mu_h]]. \tag{78}$$

We note that $E_{2,e}$ and $E^{\mathrm{in}}_{2,e}$ have the same dimension. Here, we introduced the notation Γ^{in}_e for the *inter-element* part of the element boundary Γ_e, i.e. the part of Γ_e that does not intersect with the exterior boundary Γ. Moreover $[[\cdot]]$ denotes the jump across an element boundary. More precisely, $[[\mu]] = \mu^+ - \mu^-$, where μ^+ is the value in the neighboring element, whereas μ^- is the value in Ω_e. Apparently, the residual errors $\hat{R}_1$, $\hat{\boldsymbol{R}}_2$ and $\hat{R}^{\mathrm{in}}_2$ are computable from the finite element solutions μ_h and $\boldsymbol{g}_h$.

Henceforth, we shall consider the special element approximation (CL), defined above, with piecewise constant μ_h and piecewise linear (but continuous) $\boldsymbol{g}_h$. We then conclude that

$$\hat{R}_1 = 0, \qquad \hat{\boldsymbol{R}}_2 = (\boldsymbol{H}^{\mathrm{g}})^{-1} \cdot \boldsymbol{g}_h, \tag{79}$$

where it was used that $\nabla \mu_h = 0$ on Ω_e. Moreover, the jump term $\hat{R}^{\mathrm{in}}_2$, which is piecewise constant on each inter-element part of Γ_e, represents (in some sense) the "gradient of μ_h" and thereby replaces the term $-\nabla \mu_h$ for this choice of approximation. We thus obtain the reduced (but still exact) error representation:

$$e^2_{\mathrm{E}} = \sum_{e=1}^{N} \left(E_{2,e} + E^{\mathrm{in}}_{2,e} \right). \tag{80}$$

We shall now endeavor to find a function $\boldsymbol{r} \in W$ such that it satisfies the following relation on Ω_e:

$$\int_{\Omega_e} \boldsymbol{r} \cdot \boldsymbol{e}_g \,\mathrm{d}\Omega = \int_{\Omega_e} \hat{\boldsymbol{R}}_2 \cdot \boldsymbol{e}_g \,\mathrm{d}\Omega + \int_{\Gamma^{\mathrm{in}}_e} h_e \hat{R}^{\mathrm{in}}_2 \boldsymbol{n} \cdot \boldsymbol{e}_g \,\mathrm{d}\Gamma. \tag{81}$$

To this end, we consider the more general problem of finding $\boldsymbol{r} \in W$ such that

$$\int_{\Omega_e} \boldsymbol{r} \cdot \boldsymbol{g}' \,\mathrm{d}\Omega = \int_{\Omega_e} \hat{\boldsymbol{R}}_2 \cdot \boldsymbol{g}' \,\mathrm{d}\Omega + \int_{\Gamma^{\mathrm{in}}_e} h_e \hat{R}^{\mathrm{in}}_2 \boldsymbol{n} \cdot \boldsymbol{g}' \,\mathrm{d}\Gamma, \quad \forall \boldsymbol{g}' \in W. \tag{82}$$

Clearly, on setting $\boldsymbol{g}' = \boldsymbol{e}_g$ in Eq. (82), we obtain the error representation Eq. 81. Approximating $\boldsymbol{r}$ in the finite element sense (rather than solving for $\boldsymbol{r}$ exactly), we look for $\boldsymbol{r}_h \in W_h$ such that

$$\int_{\Omega_e} \boldsymbol{r}_h \cdot \boldsymbol{g}'_h \,\mathrm{d}\Omega = \int_{\Omega_e} \hat{\boldsymbol{R}}_2 \cdot \boldsymbol{g}'_h \,\mathrm{d}\Omega + \int_{\Gamma^{\mathrm{in}}_e} h_e \hat{R}^{\mathrm{in}}_2 \boldsymbol{n} \cdot \boldsymbol{g}'_h \,\mathrm{d}\Gamma, \quad \forall \boldsymbol{g}'_h \in W_h. \tag{83}$$

Clearly, $\boldsymbol{r}_h$ approximates $\boldsymbol{r}$ in the "best way" since $\boldsymbol{r}_h$ is the projection of $\boldsymbol{r}$ onto the space W_h, i.e. $(\boldsymbol{r} - \boldsymbol{r}_h, \boldsymbol{g}'_h)_{L_2(\Omega_e)} = 0$ for all $\boldsymbol{g}'_h \in W_h$.

We are now in the position to evaluate the element error as follows:

$$e^2_{\mathrm{E}(\Omega_e)} = -l^2 \int_{\Omega_e} \boldsymbol{r} \cdot \boldsymbol{e}_g \,\mathrm{d}\Omega \simeq -l^2 \int_{\Omega_e} \boldsymbol{r}_h \cdot \boldsymbol{e}_g \,\mathrm{d}\Omega = -l^2 \int_{\Omega_e} \bar{\boldsymbol{r}}_h \cdot (\boldsymbol{H}^{\mathrm{g}})^{-1} \cdot \boldsymbol{e}_g \,\mathrm{d}\Omega, \tag{84}$$

where we introduced $\bar{\boldsymbol{r}}_h = \boldsymbol{H}^{\mathrm{g}} \cdot \boldsymbol{r}_h$. Using Cauchy–Schwartz' inequality, we now obtain

$$e^2_{\mathrm{E}(\Omega_e)} \leqslant l^2 \|\bar{\boldsymbol{r}}_h\|_{C(\Omega_e)} \|\boldsymbol{e}_g\|_{C(\Omega_e)}. \tag{85}$$

However, from Eq. (73), we have the trivial estimate

$$l\|\boldsymbol{e}_g\|_{C(\Omega_e)} \leqslant e_{\mathrm{E}(\Omega_e)} \tag{86}$$

which can be combined with Eq. (85) to give

$$e_{\mathrm{E}(\Omega_e)} \leqslant l\|\bar{\boldsymbol{r}}_h\|_{C(\Omega_e)} \rightsquigarrow e_{\mathrm{E}} \leqslant l\|\bar{\boldsymbol{r}}_h\|_C, \tag{87}$$

where it is recalled that

$$\|\bar{\boldsymbol{r}}_h\|_C = \left(\sum_{e=1}^{N} \int_{\Omega_e} \bar{\boldsymbol{r}}_h \cdot (\boldsymbol{H}^{\mathrm{g}})^{-1} \cdot \bar{\boldsymbol{r}}_h \,\mathrm{d}\Omega\right)^{1/2} = \left(\sum_{e=1}^{N} \int_{\Omega_e} \boldsymbol{r}_h \cdot \boldsymbol{H}^{\mathrm{g}} \cdot \boldsymbol{r}_h \,\mathrm{d}\Omega\right)^{1/2}. \tag{88}$$

It is remarked that this error estimate, which provides a strict upper bound if we disregard the approximation $\boldsymbol{r} \to \boldsymbol{r}_h$ in Eq. (84), *does not involve any interpolation* (or other) constants. This estimate is rather of the Z^2-type (cf. Zienkiewicz and Zhu, 1987), in the sense that $\boldsymbol{r}_h$ represents the difference between $(\boldsymbol{H}^{\mathrm{g}})^{-1} \cdot \boldsymbol{g}_h$ and the "gradient of μ_h" expressed as $\hat{R}_2^{\mathrm{in}}$ (cf. Hansbo and Runesson, 1999).

In an adaptive strategy, we shall try to equidistribute the error over $\mathscr{M}_h$, i.e. the contribution to e_{E}^2 from each Ω_e should be equal. Hence, we would have in such an optimal situation

$$e_{\mathrm{E}}^2 \leqslant \sum_{e=1}^{N} l^2 \int_{\Omega_e} \boldsymbol{r}_h \cdot \boldsymbol{H}^{\mathrm{g}} \cdot \boldsymbol{r}_h \,\mathrm{d}\Omega \leqslant \sum_{e=1}^{N} l^2 r_e A_e \simeq N l^2 r_e h_e^2, \tag{89}$$

where $A_e \sim h_e^2$ is the area of Ω_e and

$$r_e = \max_{\boldsymbol{x} \in \Omega_e} (|\boldsymbol{r}_h \cdot \boldsymbol{H}^{\mathrm{g}} \cdot \boldsymbol{r}_h|). \tag{90}$$

From the stopping criterion $e_{\mathrm{E}} \leqslant \mathrm{TOL}$, where TOL is a given tolerance, we establish the recursion formula for the jth mesh refinement:

$$h_e^{(j+1)} \simeq \frac{\mathrm{TOL}}{l\sqrt{N^{(j)} r_e^{(j)}}}. \tag{91}$$

Remark 8. *Recall the exact error representation*

$$e_{\mathrm{E}}^2 = -\sum_{e=1}^{N} l^2 \int_{\Omega_e} \boldsymbol{r} \cdot \boldsymbol{e}_g \,\mathrm{d}\Omega \tag{92}$$

It appears that $e_{\mathrm{E}} = 0$ *when*

- $l = 0$ (*local theory*),
- $\boldsymbol{g}_h = 0$, $\mu_h = const$ (*homogeneous solution*) $\rightsquigarrow \hat{\boldsymbol{R}}_2 = 0$, $\hat{R}_2^{\mathrm{in}} = 0 \rightsquigarrow \boldsymbol{r} = 0$.

With mesh refinement, we expect $\boldsymbol{r} \to 0$ ($\boldsymbol{r}_h \to 0$) *with the following motivation*: *Recalling Eq.* (92) *with Eq.* (81):

$$e_{\mathrm{E}}^2 = -l^2 \sum_{e=1}^{N} \left(\int_{\Omega_e} \hat{\boldsymbol{R}}_2 \cdot \boldsymbol{e}_g \,\mathrm{d}\Omega + \int_{\Gamma_e^{\mathrm{in}}} \hat{R}_2^{\mathrm{in}} \boldsymbol{n} \cdot \boldsymbol{e}_g \,\mathrm{d}\Gamma \right) \tag{93}$$

However, the Galerkin orthogonality in Eqs. (50) *and* (51) gives

$$\sum_{e=1}^{N} \left(\int_{\Omega_e} \hat{\boldsymbol{R}}_2 \cdot \boldsymbol{g}_h' \,\mathrm{d}\Omega + \int_{\Gamma_e^{\mathrm{in}}} \hat{R}_2^{\mathrm{in}} \boldsymbol{n} \cdot \boldsymbol{g}_h' \,\mathrm{d}\Gamma \right) = 0, \quad \forall \boldsymbol{g}_h' \in W_h. \tag{94}$$

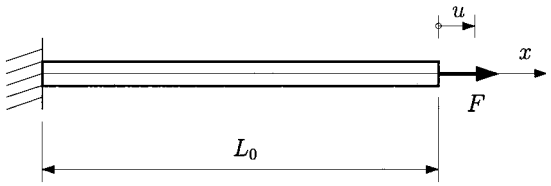

Fig. 1. One-dimensional tension bar.

Table 1
Material parameters for one-dimensional problems

Common parameters	Softening plasticity	Plasticity and damage
$E = 1000\sigma_y, \quad \nu = 0.3$	$H = -30\sigma_y$	$H = 100\sigma_y$
$H^g = \lvert H\rvert/(4\pi^2)$	$K_\infty = \infty$	$K_\infty = 1.0\sigma_y$
$l = 0.3$ m	$S = \infty$	$S = 5 \times 10^{-5}\sigma_y$
$L_0 = 1.0$ m		$m = 1$

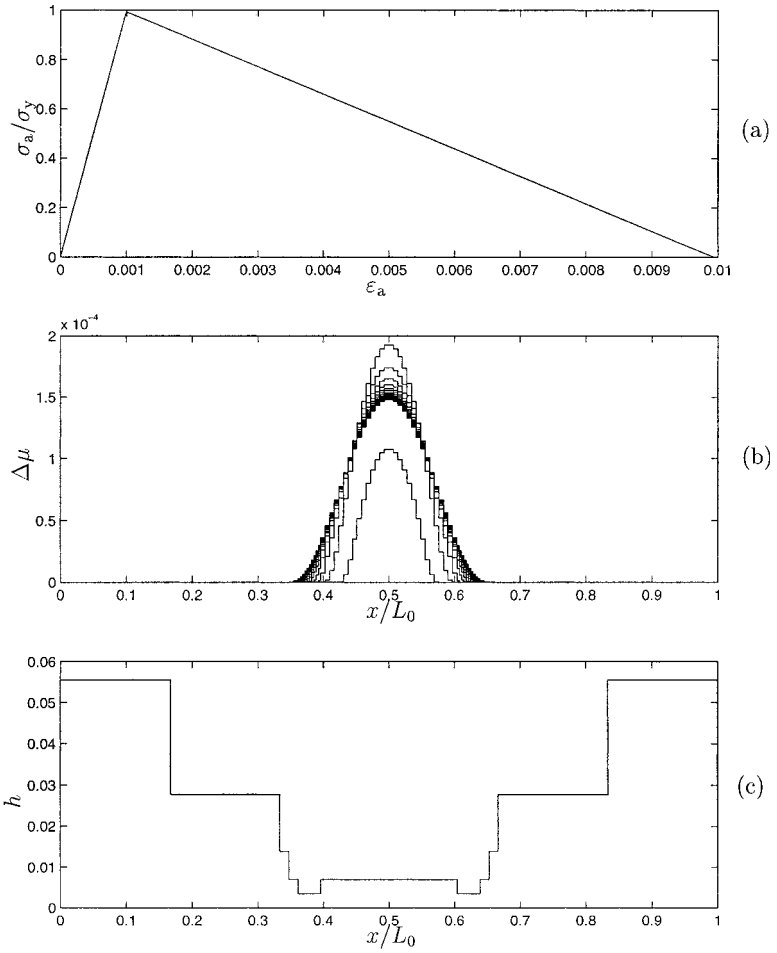

Fig. 2. Results for adaptive meshes (softening plasticity): (a) load versus average strain, (b) currently active plastic zone, and (c) mesh function in last loadstep.

When the mesh is refined, i.e. the space W_h is enlarged, we expect $\boldsymbol{e}_g$ to be approximated closely with some $\boldsymbol{g}'_h \in W_h$ and so it follows that $e_E \to 0$.

5. Numerical examples

5.1. One-dimensional tension bar

As a first example showing the behavior of the suggested adaptive numerical method, we examine the one-dimensional tension bar in Fig. 1. The bar is fixed at one end and subjected to prescribed displacement at the other. A small weakness (1%) is introduced in one element at the center of the bar. The relevant material parameters are given in Table 1 for two different material models: (1) softening plasticity (without damage) and (2) hardening plasticity coupled to damage development. For both the material models, we

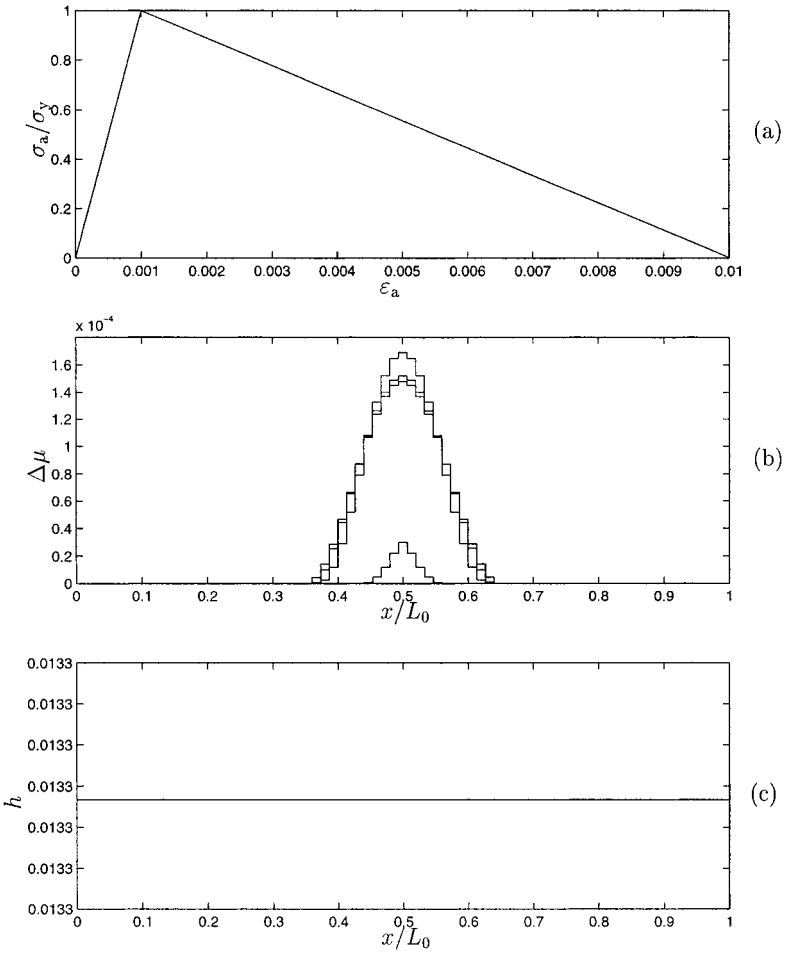

Fig. 3. Results for uniform mesh (softening plasticity): (a) load versus average strain, (b) currently active plastic zone, and (c) mesh function.

apply a loading sequence consisting of equal increments of prescribed end displacement Δu, which corresponds to the "average strain" increment $\Delta\varepsilon_a = \Delta u/L_0 = 2 \times 10^{-5}$.

We first consider the softening plasticity model. Fig. 2a and b show the result that is obtained from the adaptive mesh in each loadstep (which is optimal in the sense that the error is equidistributed within the currently active plastic zone). The mesh function for the adaptive mesh in the last step is shown in Fig. 2c. Starting from nine equal elements ($N^{(0)} = 9$, $h_e^{(0)} = 0.111$ m), we needed 12 remeshings to obtain this mesh, which has 74 elements ($N^{(12)} = 74$) and corresponds to the estimated error $e_E^{(12)} = 2.28 \times 10^{-9}$. It is seen in Fig. 2b that the size of the current plastic zone remains virtually constant as deformation progresses. The result of the adaptive meshes is compared to that of a uniform mesh with $N = 75$ *equal* elements in Fig. 3. In this case, the error in the last loadstep becomes $e_E = 9.07 \times 10^{-9}$, which is significantly larger than for the optimal mesh.

A similar series of computations were carried out for hardening plasticity with kinetic coupling to damage. Fig. 4 shows the results of adaptive meshes. In particular, Fig. 4b shows how the localization zone is completely diffused at the onset of localization and then becomes narrower with increasing deformation,

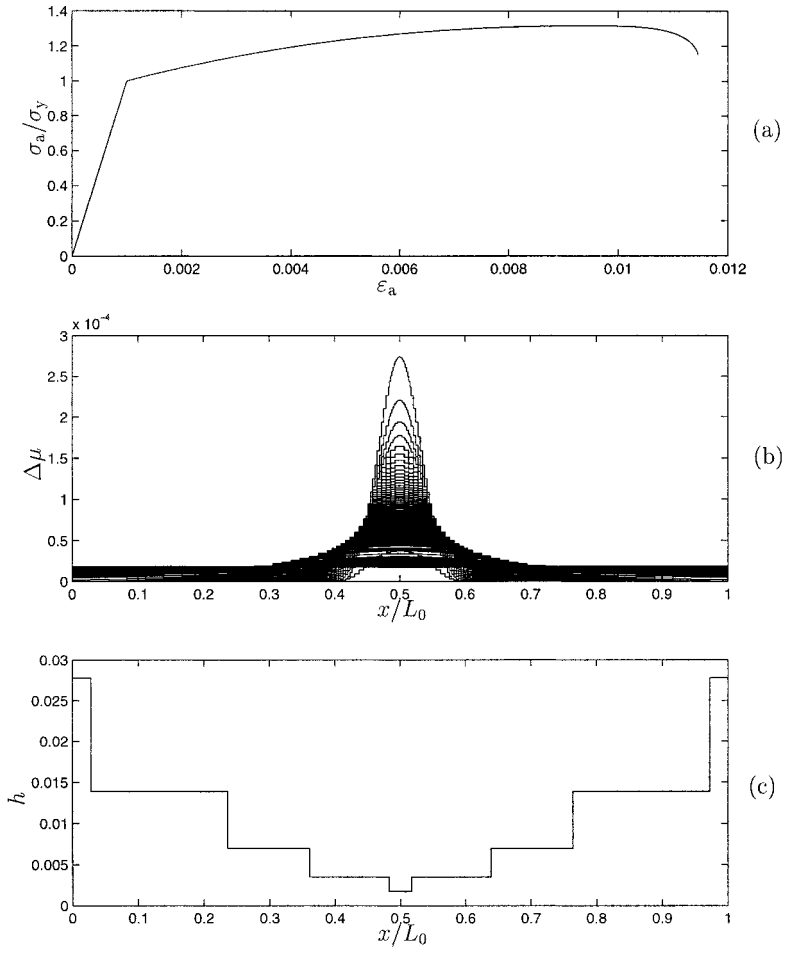

Fig. 4. Results for adaptive meshes (hardening plasticity with damage): (a) load versus average strain, (b) currently active plastic zone, and (c) mesh function in last loadstep.

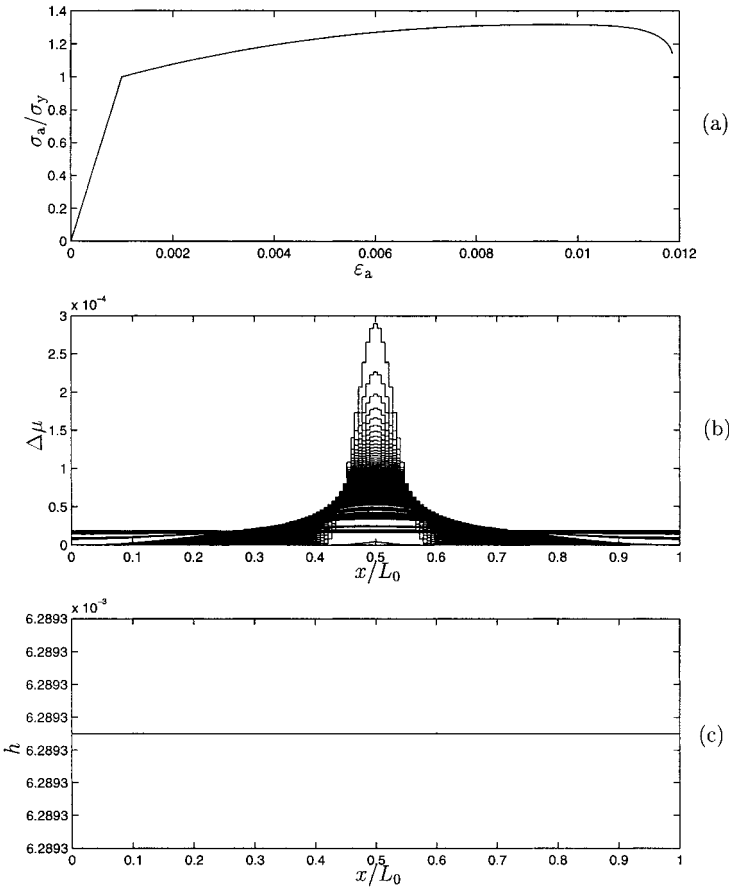

Fig. 5. Results for uniform mesh (hardening plasticity with damage): (a) load versus average strain, (b) currently active plastic zone, and (c) mesh function.

thus requiring adaptive remeshing in order to resolve the physical behavior. Fig. 4c shows the mesh function in the last loadstep just before the calculation stopped because of too rapid damage growth in the localization zone. Again, starting from $N^{(0)} = 9$ in this step, we needed 46 remeshings to obtain $N^{(46)} = 158$ corresponding to $e_E^{(46)} = 2.24 \times 10^{-9}$. Finally, a comparison was made with a uniform mesh with $N = 159$ elements in Fig. 5. The error for this mesh in the last step was $e_E = 1.42 \times 10^{-8}$, which is an order of magnitude larger than for the optimal mesh. Moreover, it is noted that the stress–strain response, as shown in Fig. 5a, is more ductile than that of the adaptive mesh in Fig. 4a. This reflects the fact that the localization cannot be resolved appropriately with the uniform mesh.

5.2. Rectangular plate in plane strain

Numerical simulations of the localization characteristics were carried out for the rectangular plate in plane strain, shown in Fig. 6. The plate is subjected to uniform prescribed vertical displacement along its top edge, while the bottom edge is kept straight. Both edges can only transmit normal forces (perfectly smooth boundaries). The prelocalized state is thus characterized as uniaxial strain/stress. Localization is triggered by a slight reduction of σ_y (in a few elements) at the center of the plate.

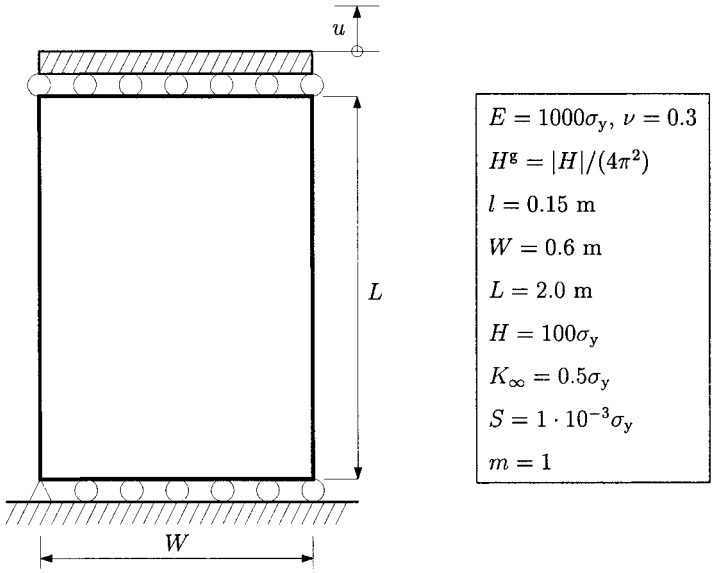

Fig. 6. Homogenous rectangular plate (subjected to prescribed end displacement) and used material parameters.

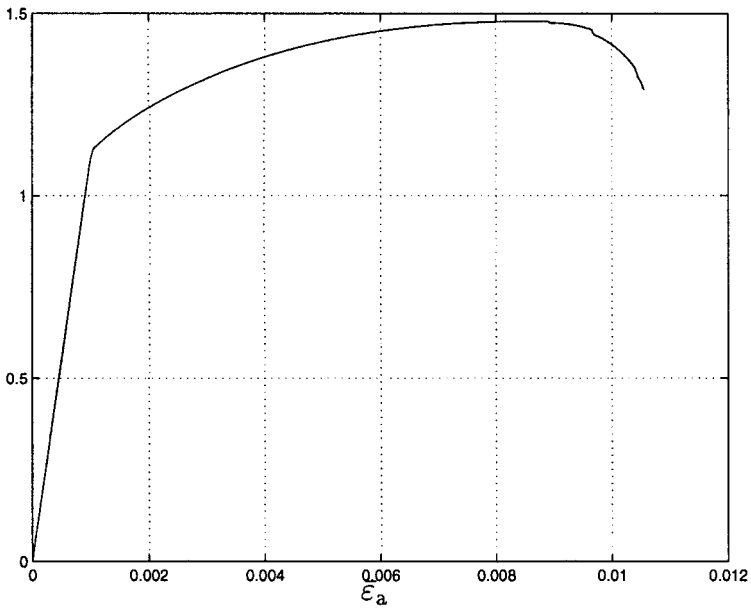

Fig. 7. Load versus average strain.

The critical state will occur first after significant accumulation of damage corresponding to an *initially diffuse* localization zone. Like for the tension bar, it is concluded that the width of the localization zone gradually decreases, cf. the results in Figs. 7–10. In particular, Fig. 9 shows how the currently active plastic zone (within which $\Delta\mu > 0$) decreases with increasing overall deformation. All results are shown for adaptive meshes with equidistributed error within the current plastic zone. The mesh density itself gives a

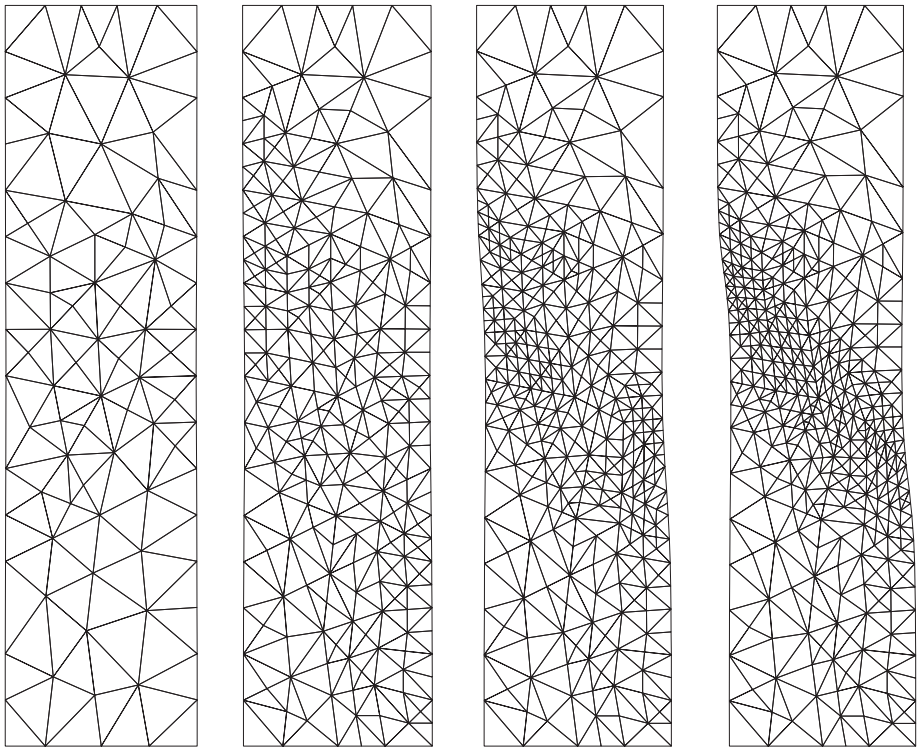

Fig. 8. Displacement patterns (and adaptive meshes) for $\bar{\varepsilon}_a = 0.008$, 0.009, 0.010 and after the last loadstep (displacements are magnified 10 times).

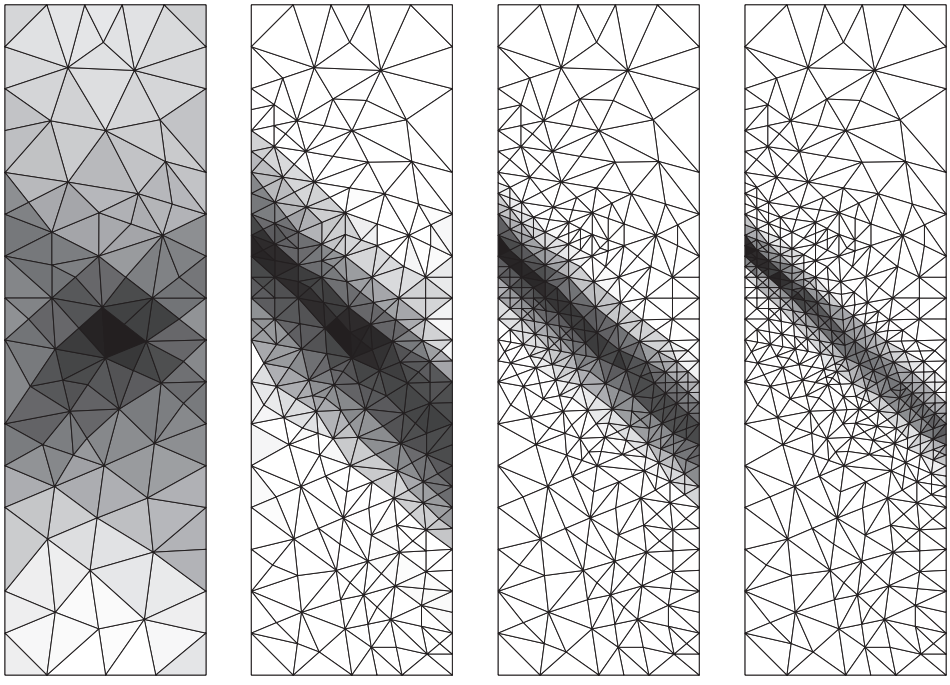

Fig. 9. Magnitude of incremental plastic strain (in terms of the plastic multiplier increment $\Delta\mu$) for $\bar{\varepsilon}_a = 0.008$, 0.009, 0.010 and in the last loadstep.

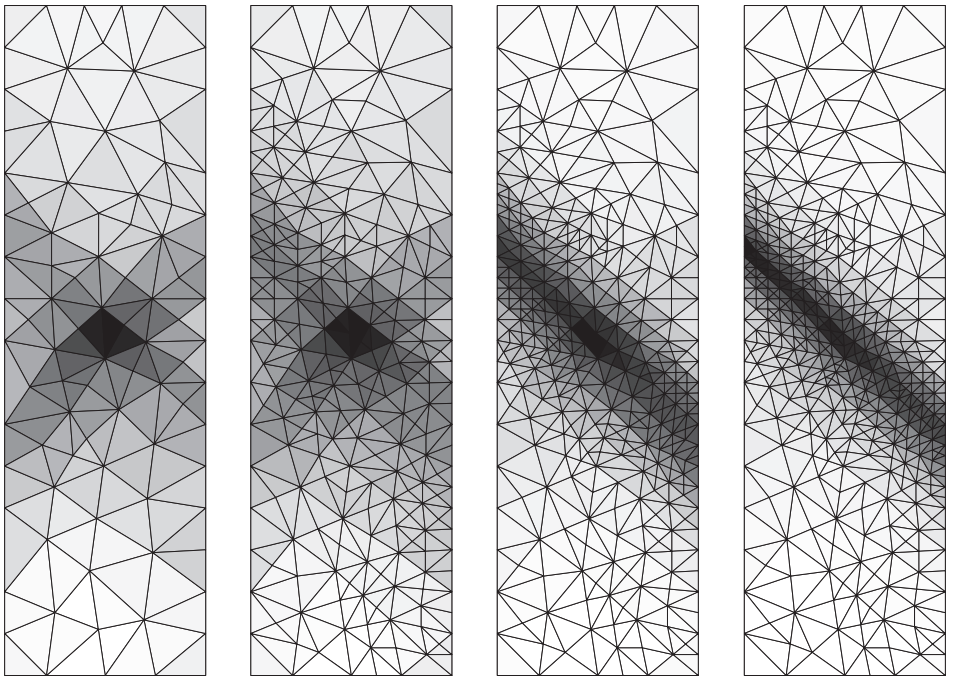

Fig. 10. Magnitude of accumulated plastic strain (in terms of the total plastic multiplier μ) for $\bar{\varepsilon}_a = 0.008, 0.009, 0.010$ and after the last loadstep.

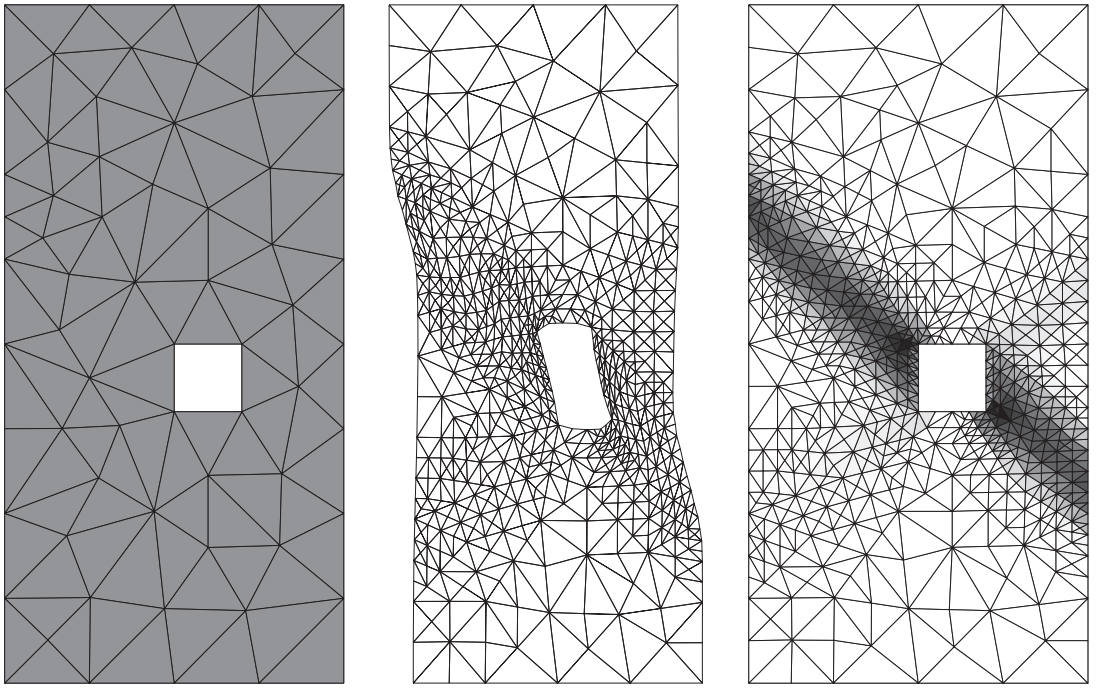

Fig. 11. Initial mesh (with 101 elements), displacement (magnified 100 times) (with 1217 elements) and magnitude of accumulated plastic strain (in terms of the total plastic multiplier μ) of final mesh.

good impression of the localized solution, both in terms of the total deformation (Fig. 8) and the plastic deformation (Figs. 9 and 10).

To verify that the adaptive method also works for nonhomogenous conditions (prior to plastic deformation, i.e., after plastic deformation, the state is nonhomogenous even for the example above), a slightly modified problem was studied. The plate in Fig. 6 was modified with $W = 1.0$ m and a square hole with side length 0.2 m and its upper left corner at the center of the plate. The material parameters were chosen to represent linear softening with $H = -50\sigma_y$ and $l = 0.3$ m. The results are shown in Fig. 11.

6. Concluding remarks

It is possible to device an adaptive strategy for gradient theory of plasticity based on the constitutive subproblem with the plastic multiplier as the primary unknown. It appears that the adaptive meshes do indeed represent the localization features of the deformation field. The underlying a posteriori error estimate is expressed for the energy norm of the plastic multiplier increment in each load (or time) step. Moreover, in this paper, we have considered only the error distribution in space (and not its evolution in time). A more comprehensive analysis must include the error from the equilibrium equation as well as the error in space time. The proposed technique seems to be useful as a step towards this general strategy.

References

Belytschko, T., Tabbara, M., 1993. H-adaptive finite element methods for dynamic problems, with emphasis on localization. Int. J. Num. Meth. Engng. 36, 4245–4265.

Comi, C., Corigliano, A., 1996. Uniqueness of the dynamic finite-step problem in gradient-dependent softening plasticity. Int. J. Solids Struct. 33, 3881–3902.

Comi, C., Perego, U., 1996. A generalized variable formulation for gradient dependent softening plasticity. Int. J. Num. Meth. Engng. 39, 3731–3755.

de Borst, R., Pamin, J., 1996. Some novel developments in finite element procedures for gradient-dependent plasticity. Int. J. Num. Meth. Engng. 39, 2477–2505.

Eriksson, K., Estep, D., Hansbo, P., Johnson, C., 1995. Introduction to adaptive methods for differential equations. Acta Numerica 105–158.

Hansbo, P., Runesson, K., 1999. Residual-based error estimate of the Z^2-type for elasticity. Int. J. Num. Meth. Engng., submitted for publication.

Johnson, C., Scott, R., 1981. A finite element method for problems in perfect plasticity using discontinuous trial functions. In: Wunderlich, W., Stein, E., Bathe, K.J. (Eds.), Non-linear finite element analysis in structural mechanics. Springer, Berlin. pp. 307–329.

Li, X., Cescotto, S., 1996. Finite element method for gradient plasticity at large strains. Int. J. Num. Meth. Engng. 39, 619–633.

Lorentz, E., Andrieux, S., 1999. Variational formulation for nonlocal damage models. Int. J. Plast. 15, 119–138.

Pamin, J., 1994. Gradient-dependent plasticity in numerical simulation of localization phenomena. Ph.D. Thesis, Delft University of Technology, Delft.

Sluys, L.J., de Borst, R., Mühlhaus, M., 1993. Wave propagation, localization and dispersion in a gradient-dependent medium. Int. J. Solids Struct. 30 (9), 1153–1171.

Svedberg, T., Runesson, K., 1997. A thermodynamically consistent theory of gradient-regularized plasticity coupled to damage. Int. J. Plast. 13 (6–7), 669–696.

Svedberg, T., Runesson, K., 1998. An algorithm for gradient-regularized plasticity coupled to damage based on a dual mixed FE-formulation. Comp. Meth. Appl. Mech. Engng. 161, 49–65.

Temam, R., Strang, G., 1980. Functions of bounded deformation. Arch. Ration. Mech. Anal. 75, 7–21.

Zienkiewicz, O.C., Pastor, M., Huang, M., 1995. Softening, localisation and adaptive remeshing, capture of discontinuous solutions. Comp. Mech. 17, 98–106.

Zienkiewicz, O.C., Zhu, J.Z., 1987. A simple error estimator and adaptive procedure for practical engineering analysis. Int. J. Num. Meth. Engng. 24, 337–357.